Kerastari workshop, 12-18 June 2023

Simulation-based inference for pulsar-population synthesis

Michele Ronchi, Celsa Pardo Araujo, Vanessa Graber & Nanda Rea

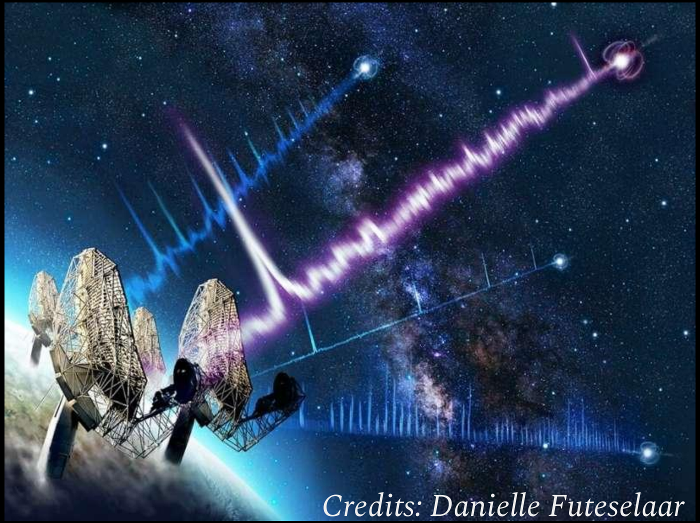

Credits: Danielle Futeselaar

ronchi@ice.csic.es
pardo@ice.csic.es
graber@ice.csic.es
rea@ice.csic.es

MAGNESIA
erc European Research Council
Established by the European Commission
Institute of Space Sciences
CSIC
Consejo Superior de Investigaciones Científicas
IEEC
EXCELENCIA MARÍA DE MAEZTU
UAB
Universitat Autònoma de Barcelona

The neutron-star zoo

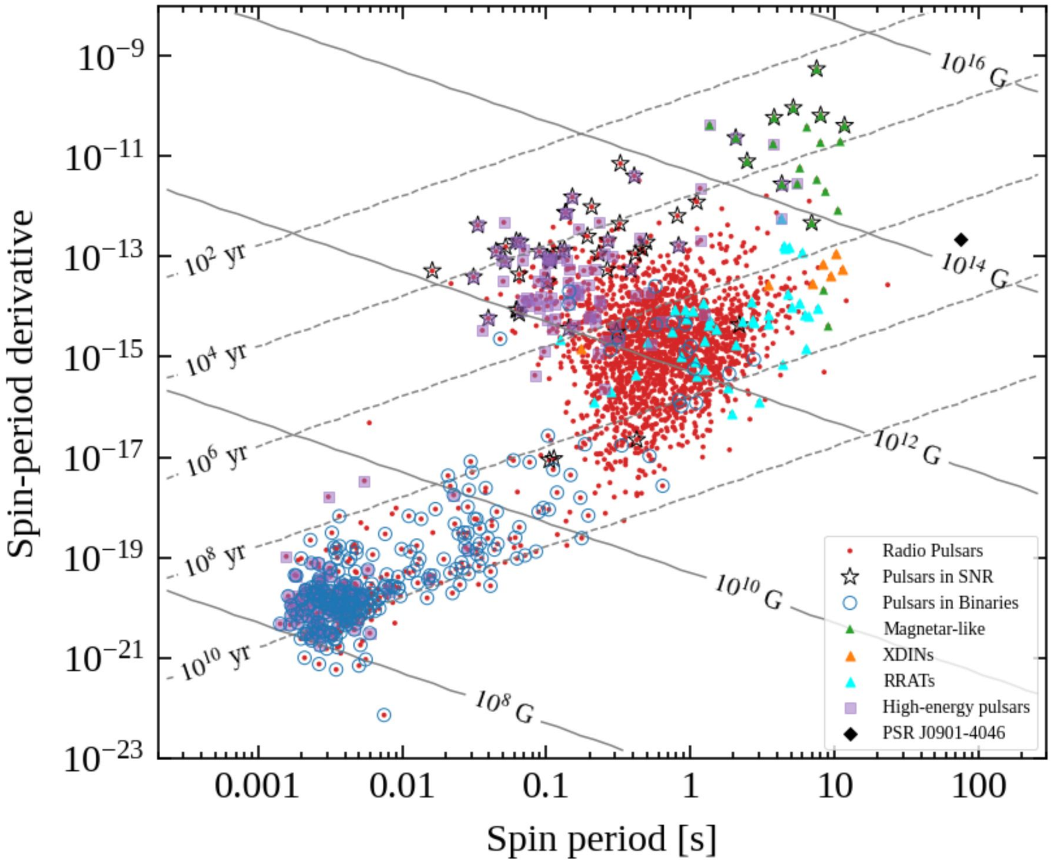

~ **3,000 pulsars** are known to date

- Neutron stars are observed as pulsars across the electromagnetic spectrum from radio to X-rays and gamma-rays
- Different classes of neutron stars occupy different locations in the $P\dot{P}$-plane probing different evolution paths and/or different origins

data from the ATNF pulsar catalogue (Manchester et al. 2005)

The neutron-star zoo

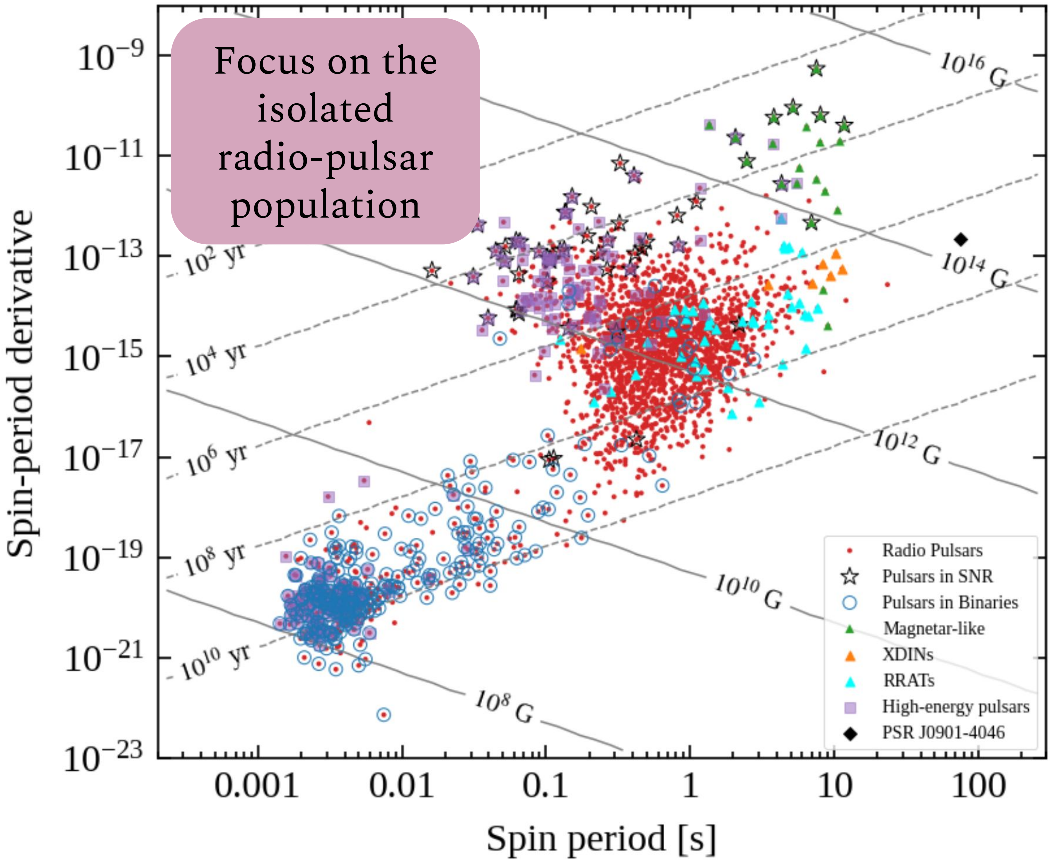

~ 3,000 pulsars are known to date

- Neutron stars are observed as pulsars across the electromagnetic spectrum from radio to X-rays and gamma-rays
- Different classes of neutron stars occupy different locations in the $P\dot{P}$-plane probing different evolution paths and/or different origins

data from the ATNF pulsar catalogue (Manchester et al. 2005)

Population synthesis

CC supernova rate:
~ 2 per century

(Rozwadowska et al. 2021)

× **Galaxy age:**
~ 13.6 billion years

= **NS number:**
~ 2.8×10^8

- We only **detect** a very **small fraction** of all neutron stars.
    - What are the **natal properties** and the **birth rate** of the NS population?
    - Is there any **evolutionary link between different neutron-star classes**?

Population synthesis

CC supernova rate:
~ 2 per century

(Rozwadowska et al. 2021)

×

Galaxy age:
~ 13.6 billion years

=

NS number:
~ 2.8×10^8

- We only **detect** a very **small fraction** of all neutron stars.
  - What are the **natal properties** and the **birth rate** of the NS population?
  - Is there any **evolutionary link between different neutron-star classes**?

- Population synthesis bridges this gap by focusing on the full population of neutron stars (e.g. Faucher-Giguère & Kaspi 2006, Lorimer et al. 2006, Gullón et al. 2014, Cieślar et al. 2020):

model **birth properties** with Monte-Carlo approach → **evolve properties** forward in time → **apply filters** to mimic observational biases/limits → **compare** mock simulations **to observations** to constrain input

ronchi@ice.csic.es

Dynamical evolution

- **Neutron stars are born in star-forming regions**, i.e., in the Galactic disk along the Milky Way's spiral arms, **and receive kicks** during the supernova explosions.

- We make the following assumptions:

    - Spiral-arm model (Yao et al. 2017) plus rigid rotation with T = 250 Myr
    - **Exponential disk model** with scale height h_c = 0.18 kpc (Wainscoat et al. 1992)
    - Single-component **Maxwell kick-velocity distribution** with dispersion σ_k = 265 km/s (Hobbs et al. 2005)
    - Galactic potential (Marchetti et al. 2019)

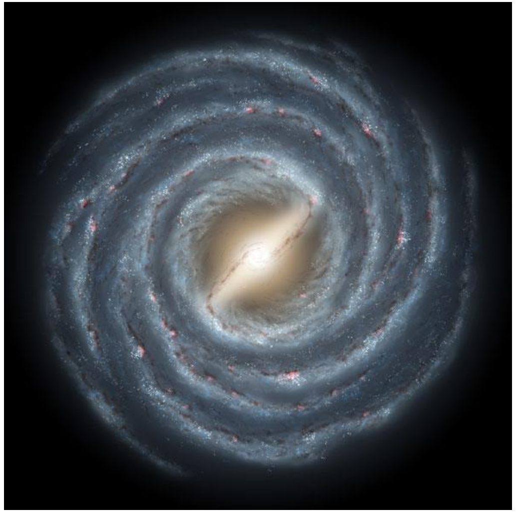

Artistic illustration of the Milky Way (credit: NASA JPL)

Dynamical evolution

- We evolve the stars' position & velocity by **solving Newtonian equations of motion** in cylindrical galactocentric coordinates:

$$\ddot{\vec{r}} = -\vec{\nabla}\Phi_{MW}$$

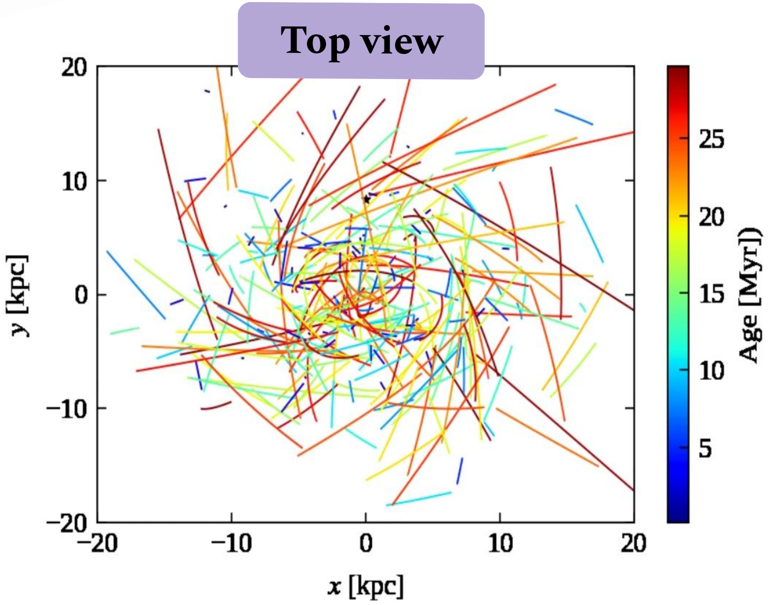

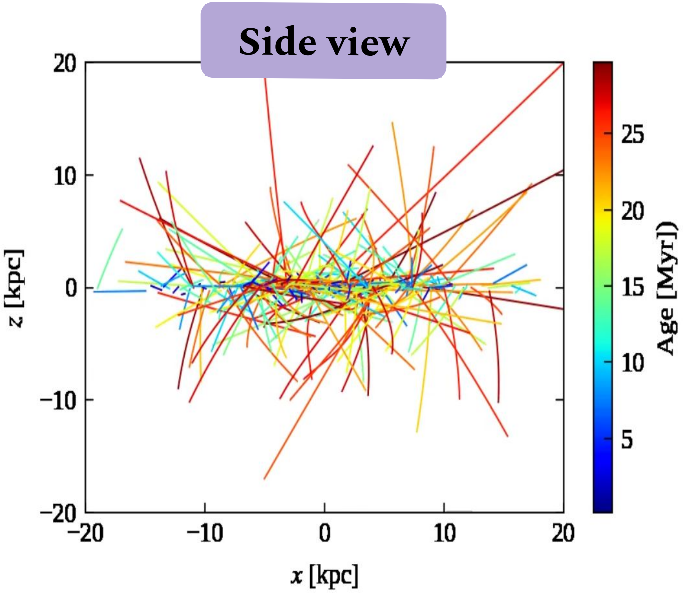

Magneto-rotational evolution

- The neutron-star magnetosphere exerts a **torque onto the star**. This causes **spin-down** and **alignment of the magnetic and rotation axes** (Spitkovsky 2006, Philippov et al. 2014).

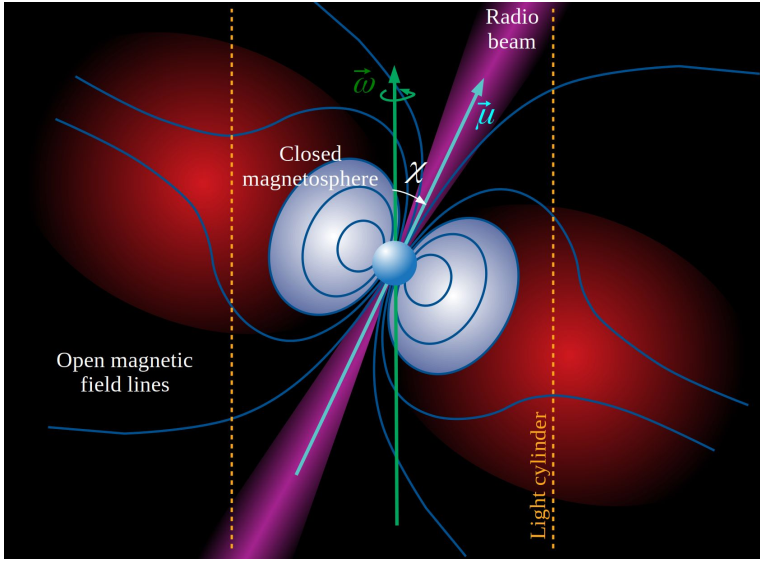

Magneto-rotational evolution

- The neutron-star magnetosphere exerts a **torque onto the star**. This causes **spin-down** and **alignment of the magnetic and rotation axes** (Spitkovsky 2006, Philippov et al. 2014).

- Neutron star **magnetic fields decay** due to the Hall effect and Ohmic dissipation in the outer stellar layer (crust) (e.g., Vigañó et al. 2013 & 2021, Gourgouliatos et al. 2014, De Grandis et al. 2020).

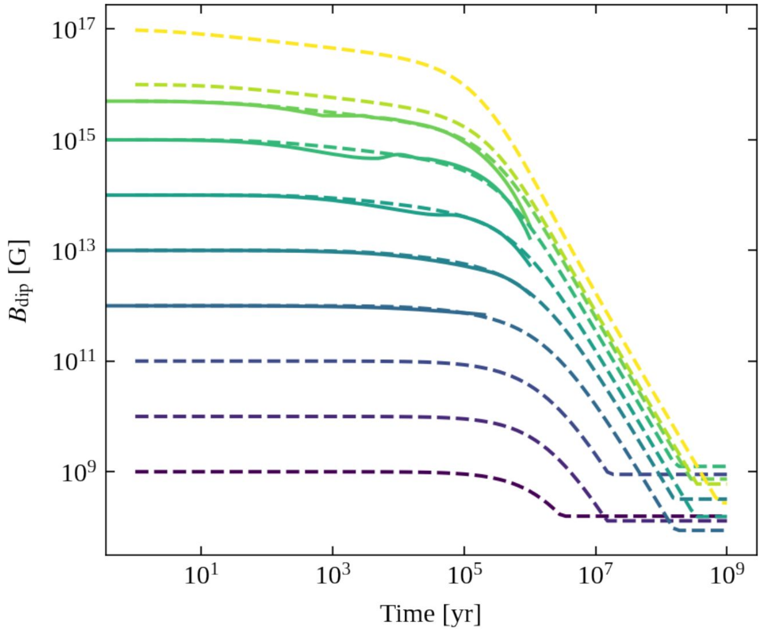

Magneto-rotational evolution

- The neutron-star magnetosphere exerts a **torque onto the star**. This causes **spin-down** and **alignment of the magnetic and rotation axes** (Spitkovsky 2006, Philippov et al. 2014).

- Neutron star **magnetic fields decay** due to the Hall effect and Ohmic dissipation in the outer stellar layer (crust) (e.g., Viganó et al. 2013 & 2021, Gourgouliatos et al. 2014, De Grandis et al. 2020).

- We make the following assumptions:
  - **Initial periods** follow a normal in log with $\mu_{\log P}$ and $\sigma_{\log P}$ (Igoshev et al. 2022)
  - **Initial fields** follow a normal in log with $\mu_{\log B}$ and $\sigma_{\log B}$ (Gullón et al. 2014)
  - **Late-time decay of the B-field** follows a power-law with index α

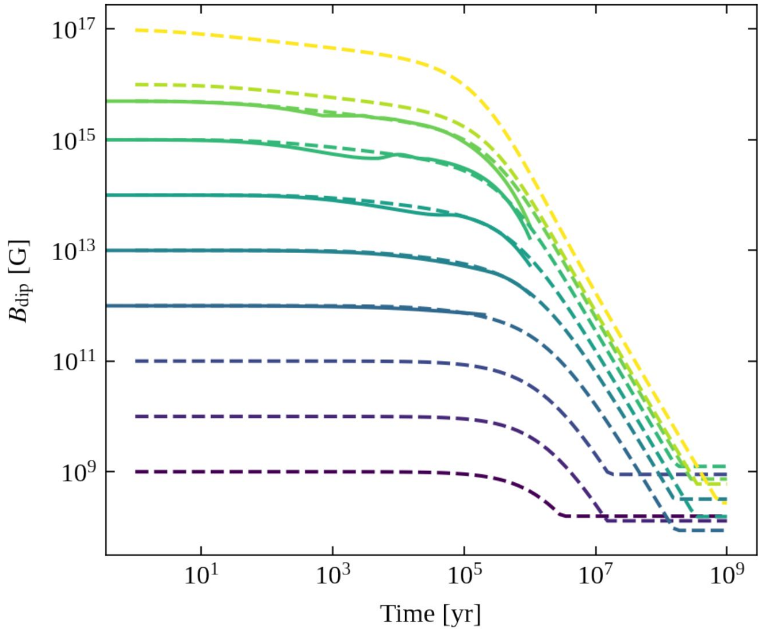

Magneto-rotational evolution

- The neutron-star magnetosphere exerts a **torque onto the star**. This causes **spin-down** and **alignment of the magnetic and rotation axes** (Spitkovsky 2006, Philippov et al. 2014).

- Neutron star **magnetic fields decay** due to the Hall effect and Ohmic dissipation in the outer stellar layer (crust) (e.g., Viganó et al. 2013 & 2021, Gourgouliatos et al. 2014, De Grandis et al. 2020).

- We make the following assumptions:
  - **Initial periods** follow a normal in log with $\mu_{\log P}$ and $\sigma_{\log P}$ (Igoshev et al. 2022)
  - **Initial fields** follow a normal in log with $\mu_{\log B}$ and $\sigma_{\log B}$ (Gullón et al. 2014)
  - **Late-time decay of the B-field** follows a power-law with index α

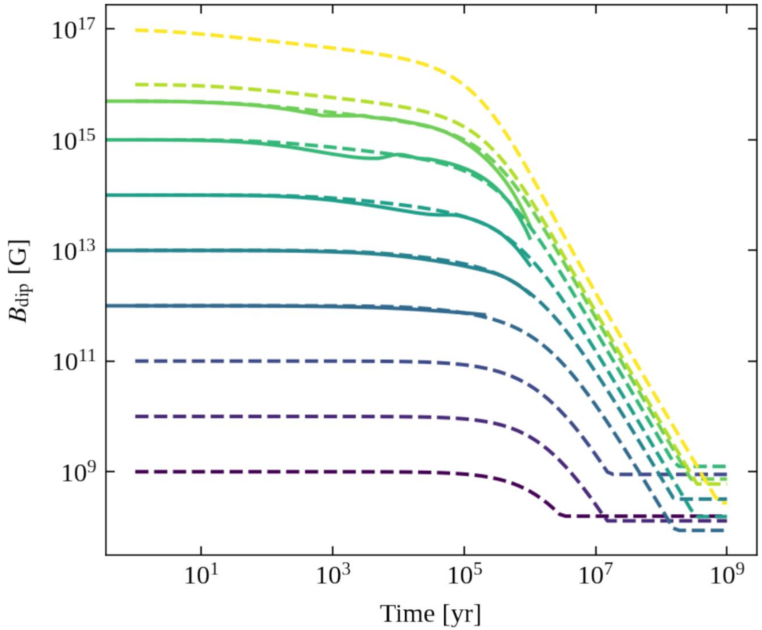

Here, we **vary** the five uncertain parameters $\boldsymbol{\mu_{\log P}}$, $\boldsymbol{\sigma_{\log P}}$, $\boldsymbol{\mu_{\log B}}$, $\boldsymbol{\sigma_{\log B}}$ and $\boldsymbol{\alpha}$.

Magneto-rotational evolution

$$\dot{P} = \frac{\pi^2}{c^3} \frac{B^2 R^6}{IP} \left(\kappa_0 + \kappa_1 \sin^2 \chi\right)$$

$$\dot{\chi} = -\frac{\pi^2}{c^3} \frac{B^2 R^6}{IP^2} \left(\kappa_2 \sin \chi \cos \chi\right)$$

(Spitkovsky 2006,
Philippov et al. 2014)

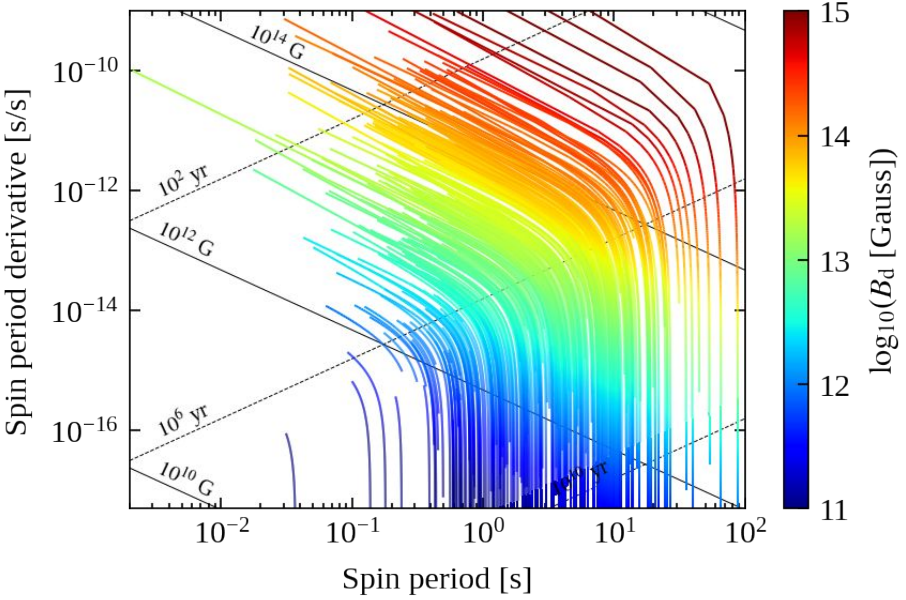

$P\dot{P}$ evolution tracks for
$\mu_{\log P}$ = -0.6 , $\sigma_{\log P}$ = 0.3 , $\mu_{\log B}$ = 13.25, $\sigma_{\log B}$ = 0.75 and α = -2.0

Radio emission and detection

- The stars' **rotational energy** E_{rot} is converted into coherent radio emission (Faucher-Giguère & Kaspi 2006; Gullón et al. 2014).

$$L_{\text{radio}} = L_0 \left(\frac{\dot{P}}{P^3} \right)^{1/2} \propto \dot{E}_{\text{rot}}^{1/2}$$

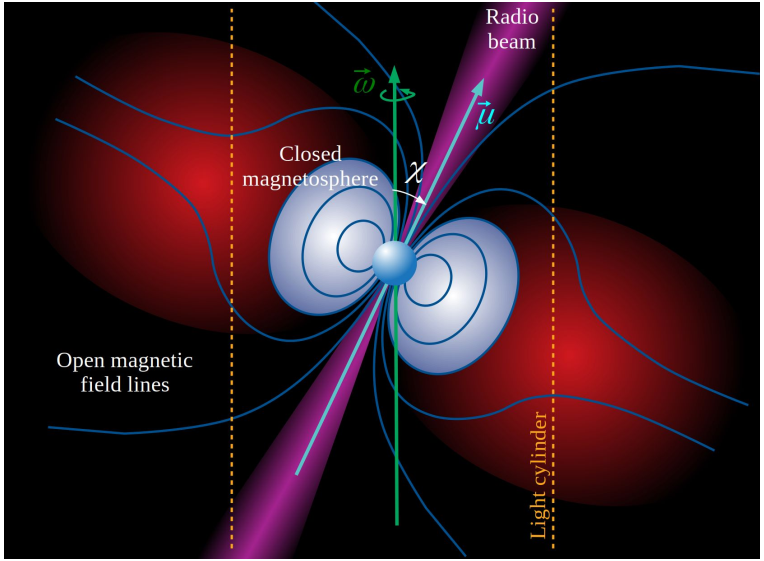

Radio emission and detection

- The stars' **rotational energy E_{rot}** is converted into coherent radio emission (Faucher-Giguère & Kaspi 2006; Gullón et al. 2014).

$$L_{\rm radio} = L_0 \left(\frac{\dot{P}}{P^3}\right)^{1/2} \propto \dot{E}_{\rm rot}^{1/2}$$

- As **emission is beamed**, ~ 90% of pulsars do not point towards us. For those intercepting our line of sight, compute **radio flux S_{radio}** & **pulse width W**.

$$S_{\rm radio} = \frac{L_{\rm radio}}{\Omega_{\rm beam} d^2}$$

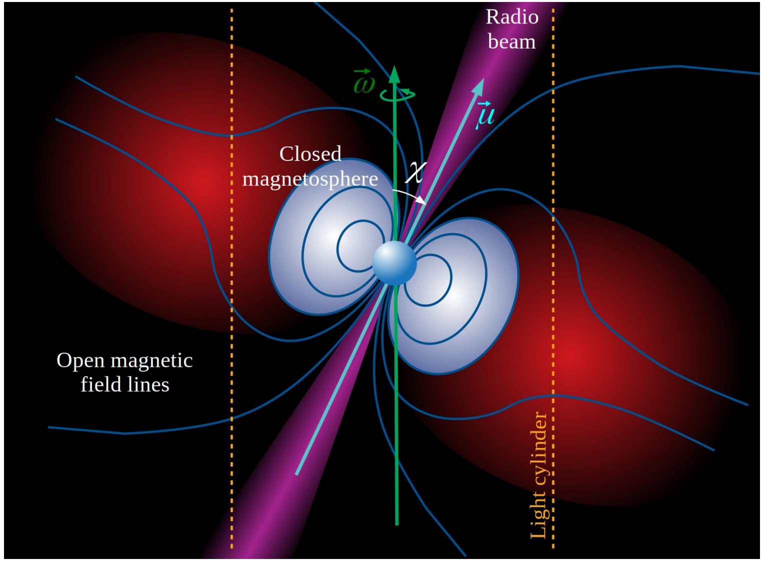

Radio emission and detection

- The stars' **rotational energy E_{rot}** is converted into coherent radio emission (Faucher-Giguère & Kaspi 2006; Gullón et al. 2014).

$$L_{\rm radio} = L_0 \left(\frac{\dot{P}}{P^3} \right)^{1/2} \propto \dot{E}_{\rm rot}^{1/2}$$

- As **emission is beamed**, ~ 90% of pulsars do not point towards us. For those intercepting our line of sight, compute **radio flux S_{radio}** & **pulse width W**.

$$S_{\rm radio} = \frac{L_{\rm radio}}{\Omega_{\rm beam} d^2}$$

- A **signal-to-noise ratio** can be estimated through the **radiometer equation**.

$$S/N = \frac{S_{\rm mean} G \sqrt{N_{\rm pol} \Delta\nu \Delta t_{\rm obs}}}{\beta \left(T_{\rm rec} + T_{\rm sky}(l,b) \right)} \sqrt{\frac{P - w_{\rm eff}}{w_{\rm eff}}}$$

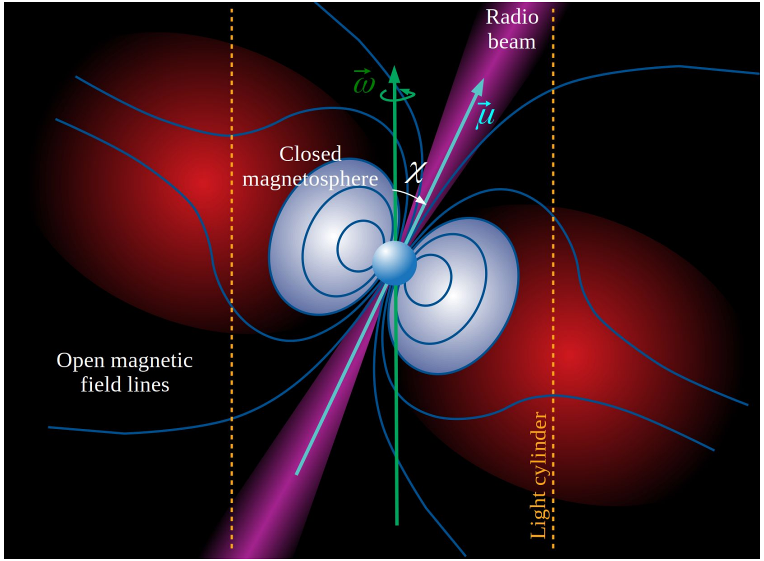

ronchi@ice.csic.es

Radio emission and detection

- The stars' **rotational energy E_{rot}** is converted into coherent radio emission (Faucher-Giguère & Kaspi 2006; Gullón et al. 2014).

$$L_{\rm radio} = L_0 \left(\frac{\dot{P}}{P^3} \right)^{1/2} \propto \dot{E}_{\rm rot}^{1/2}$$

- As **emission is beamed**, ~ 90% of pulsars do not point towards us. For those intercepting our line of sight, compute **radio flux S_{radio}** & **pulse width W**.

$$S_{\rm radio} = \frac{L_{\rm radio}}{\Omega_{\rm beam} d^2}$$

- A **signal-to-noise ratio** can be estimated through the **radiometer equation**.

$$S/N = \frac{S_{\rm mean} G \sqrt{N_{\rm pol} \Delta\nu \Delta t_{\rm obs}}}{\beta \left(T_{\rm rec} + T_{\rm sky}(l,b)\right)} \sqrt{\frac{P - w_{\rm eff}}{w_{\rm eff}}}$$

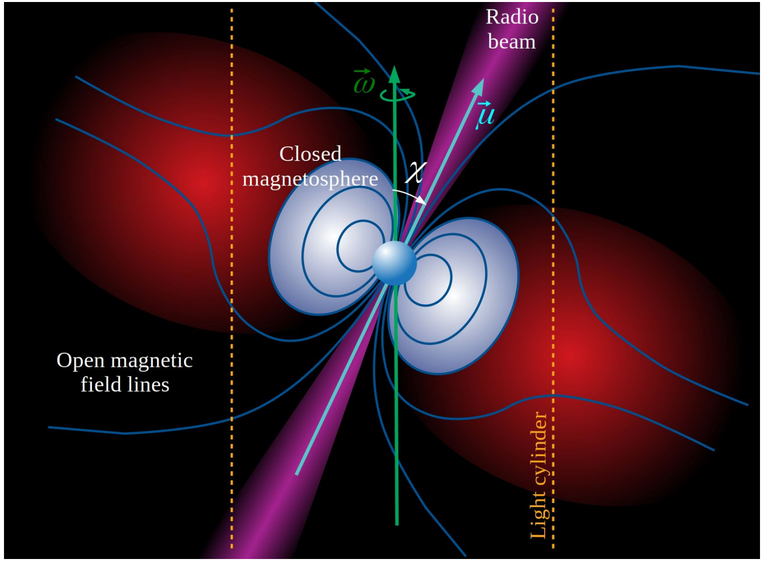

A pulsar counts as detected, if it **exceeds the sensitivity threshold** for a survey recorded with a specific radio telescope.

ronchi@ice.csic.es

Three radio surveys

- We compare our simulated populations with three surveys from Murriyang (the Parkes Radio Telescope):
  - **Parkes Multibeam Pulsar Survey** (PMPS) (Manchester et al. 2001, Lorimer et al. 2006): *1,009 isolated pulsars*
  - **Swinburne Parkes Multibeam Pulsar Survey** (SMPS) (Edwards et al. 2001, Jacoby et al. 2009): *218 isolated pulsars*
  - **High Time Resolution Universe Survey** (HTRU) (Keith et al. 2018): *1,023 isolated pulsars*

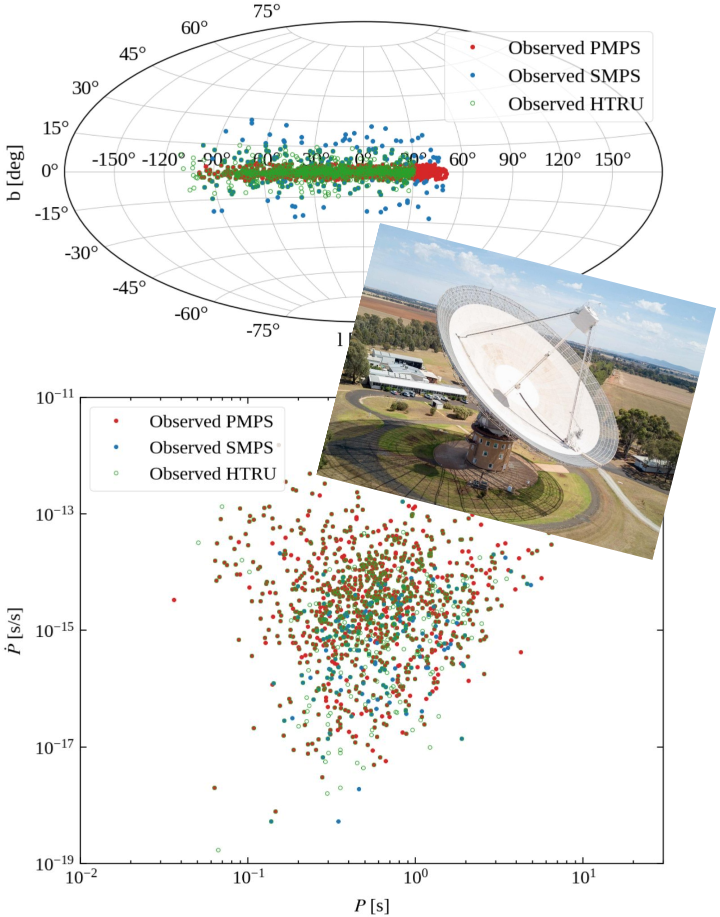

Can we constrain birth properties by looking at a current snapshot of the pulsar population?

Simulation-based (likelihood-free) inference (SBI)

- Based on some prior knowledge $\pi(\theta)$, a stochastic model and some observation x, we want to infer the most likely distribution $P(\theta|x)$ for our model parameters θ given the data x. This is **encoded in Bayes' Theorem**:

$$\underbrace{\mathcal{P}(\theta|x)}_{\text{posterior}} = \frac{\overbrace{\mathcal{P}(\theta)}^{\text{prior } \pi} \; \overbrace{\mathcal{P}(x|\theta)}^{\text{likelihood } \mathcal{L}}}{\underbrace{\mathcal{P}(x)}_{\text{evidence}}}$$

For complex simulators, the **likelihood is defined implicitly and often intractable**. This is overcome with **simulation-based** (likelihood-free) **inference** (see e.g. Cranmer et al. 2020).

- Neural Posterior Estimation (NPE) (e.g., Papamakarios & Murray 2016) uses a neural network to learn a mapping between the simulated data and the posterior distribution of the underlying parameters.

SBI - Workflow

1. **sample** θ_i from the prior $\pi(\theta)$, for $i = 1, ..., N$

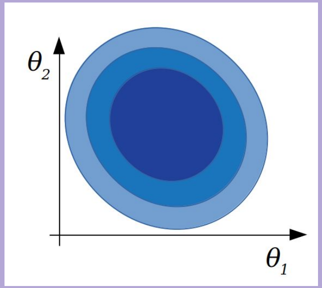

$(\mu_{\log P}, \sigma_{\log P}, \mu_{\log B}, \sigma_{\log B}, \alpha)$

SBI - Workflow

1. **sample** θ_i from the prior $\pi(\theta)$, for $i = 1, ..., N$

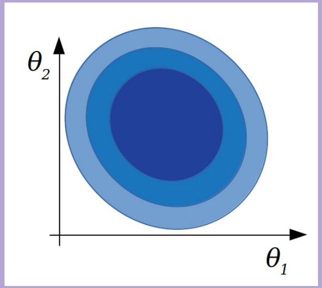

2. **run simulator** for θ_i to produce mock observations: $x_i \sim P(x|\theta_i)$

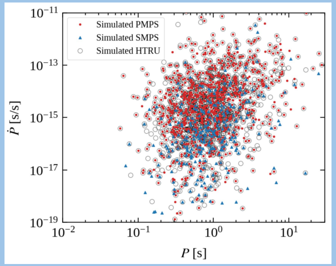

ronchi@ice.csic.es

SBI - Workflow

1. **sample** θ_i from the prior $\pi(\theta)$, for $i = 1, ..., N$

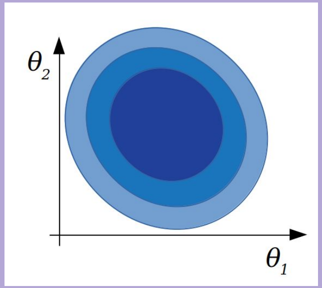

2. **run simulator** for θ_i to produce mock observations: $x_i \sim P(x|\theta_i)$

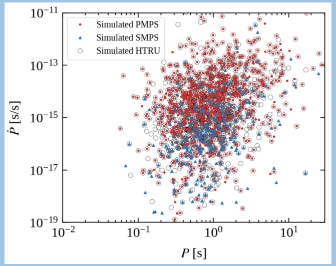

3. generate **summary statistics**: density maps of the three surveys in the $P\dot{P}$-plane

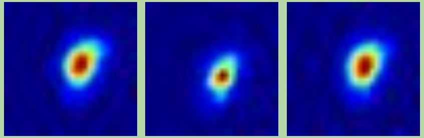

SBI - Workflow

1. **sample** θ_i from the prior $\pi(\theta)$, for $i = 1, \ldots, N$

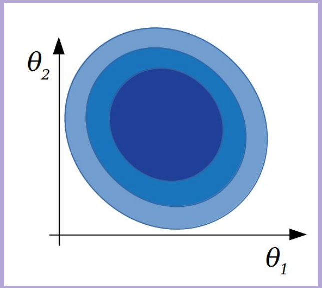

2. **run simulator** for θ_i to produce mock observations: $x_i \sim P(x|\theta_i)$

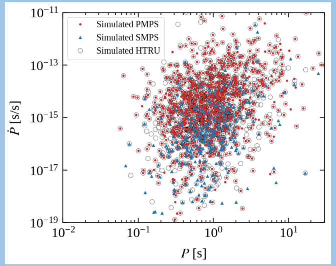

3. generate **summary statistics**: density maps of the three surveys in the $P\dot{P}$-plane

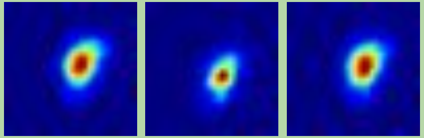

4. **train a neural network** (**conditional density estimator**) on simulated data to approximate the posterior

(Tejero-Cantero et al. 2020)

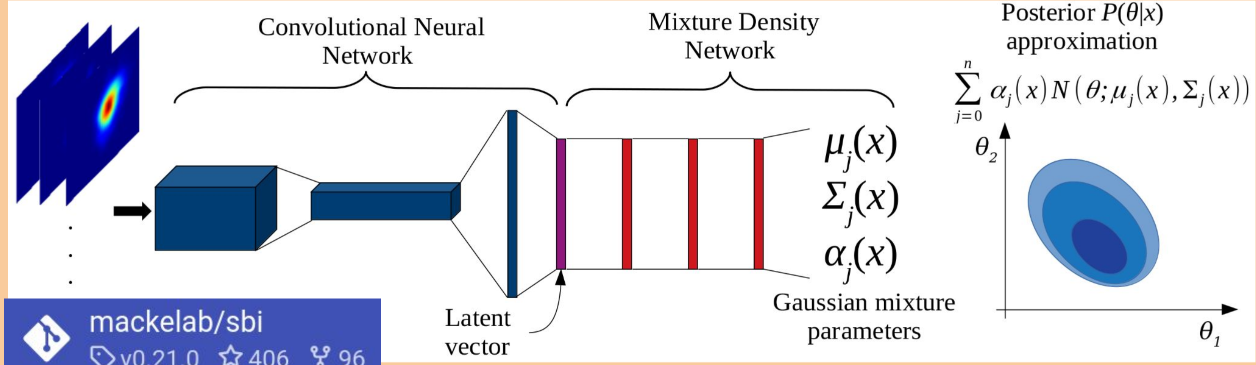

mackelab/sbi
v0.21.0 ☆ 406 96

SBI - Results

- 120,000 simulations in total, we use 87 % for training, 10 % for validation, 3 % for testing.

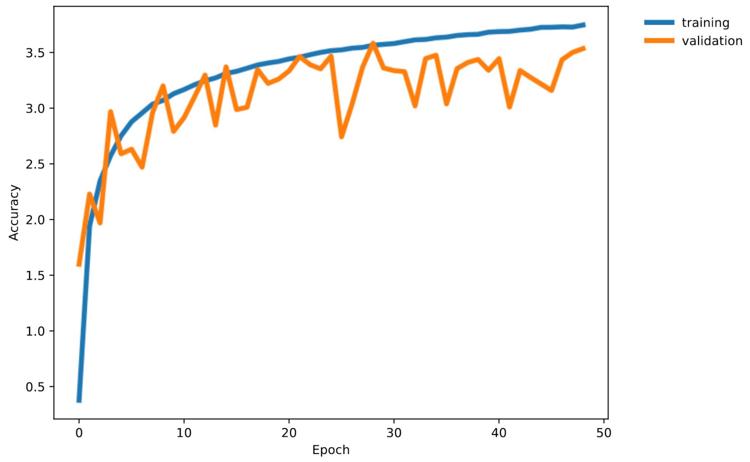

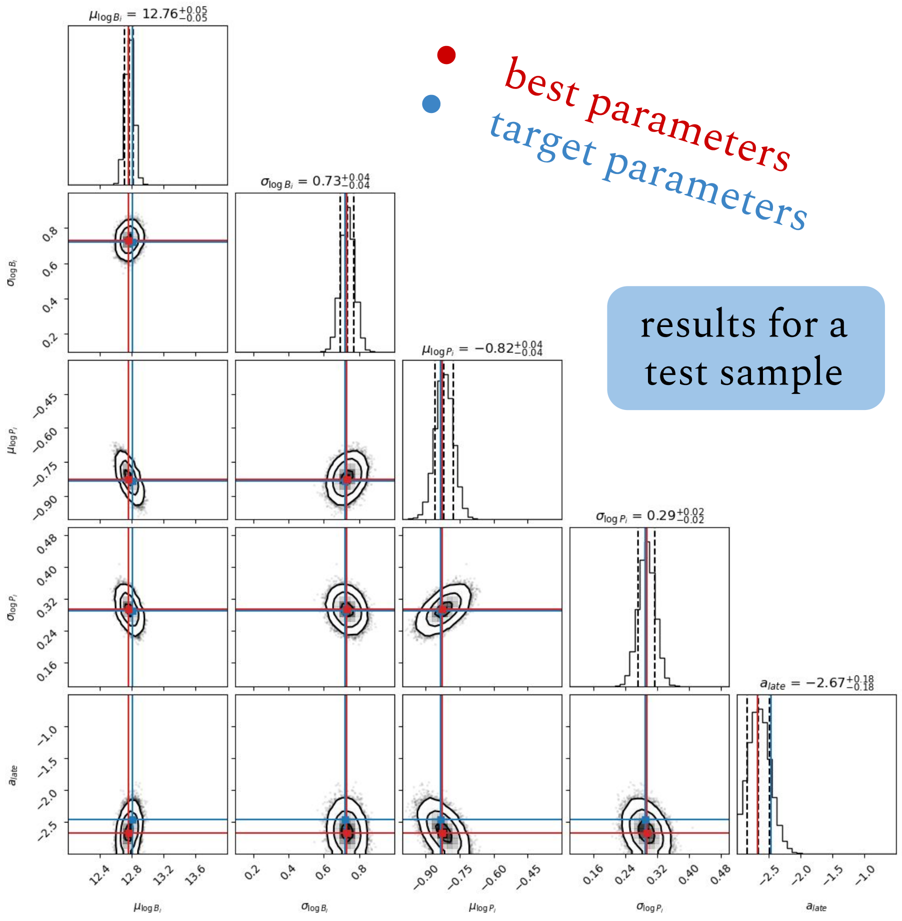

results for a test sample

The network is able to predict the posterior for any input simulation (amortized posterior).

SBI - Results for observed population

Preliminary!

With our optimised neural network, we can also **infer the posteriors** for the **pulsar population detected in our three surveys** and recover the following constraints:

$$\mu_{\log B} = 13.10^{+0.06}_{-0.06}$$
$$\sigma_{\log B} = 0.43^{+0.03}_{-0.03}$$
$$\mu_{\log P} = -0.93^{+0.12}_{-0.12}$$
$$\sigma_{\log P} = 0.40^{+0.14}_{-0.14}$$
$$\alpha = -1.92^{+0.25}_{-0.25}$$

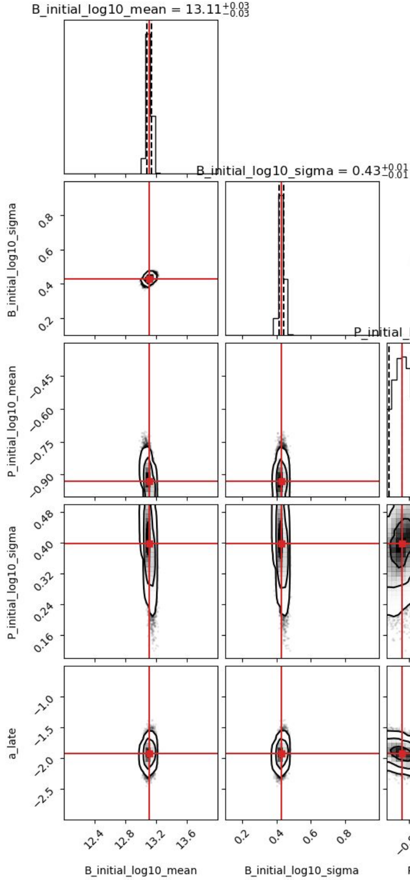

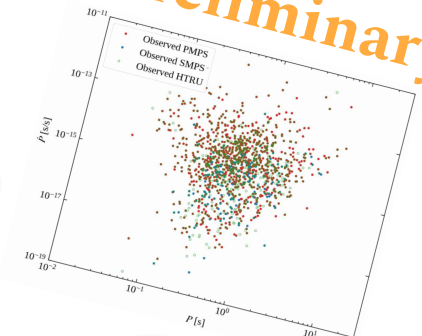

ronchi@ice.csic.es

Future plans

IMPROVING THE SIMULATOR

- Explore **different assumptions on initial** period and magnetic-field **distributions**
- Extend framework to model also gamma-ray and X-ray emission and **predict the multi-wavelength emission**

IMPROVING SBI

- Expand the approach to **active learning** and derive posteriors sequentially **using SNPE**.

Thank you!

ronchi@ice.csic.es
pardo@ice.csic.es
graber@ice.csic.es
rea@ice.csic.es

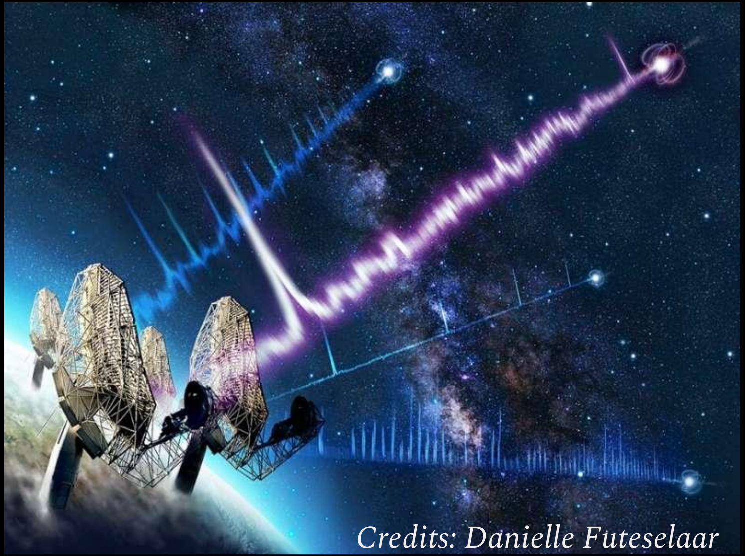

Credits: Danielle Futeselaar